Published in final edited form as:
Coord Chem Rev. 2008 February 1; 252(3-4): 444–455. doi:10.1016/j.ccr.2007.06.002.

Functional Models for the Oxygen-Evolving Complex of Photosystem II

Clyde W. Cady, **Robert H. Crabtree**, and **Gary W. Brudvig**
Department of Chemistry, Yale University, P.O. Box 208107, New Haven, CT 06520-8107, USA

Abstract

In the last ten years, a number of advances have been made in the study of the oxygen-evolving complex (OEC) of photosystem II (PSII). Along with this new understanding of the natural system has come rapid advance in chemical models of this system. The advance of PSII model chemistry is seen most strikingly in the area of functional models where the few known systems available when this topic was last reviewed has grown into two families of model systems. In concert with this work, numerous mechanistic proposals for photosynthetic water oxidation have been proposed. Here, we review the recent efforts in functional model chemistry of the oxygen-evolving complex of photosystem II.

Keywords

Oxomanganese clusters; Oxygen evolution; Ruthenium water oxidation

1. Introduction

The increasing emphasis toward “green” chemistry has intensified the search for understanding of oxygen evolution in photosynthesis, in the hope of using this information to produce artificial water-oxidation catalysts for renewable solar-energy conversion. Decades of biophysical study have provided a solid groundwork for this project. Crystal structures of photosystem II [1,2] (PSII) have revealed the location of many important components such as chlorophylls and the oxygen-evolving center (OEC) while spectroscopy such as EXAFS [3–7], EPR [8–12], and IR [13,14] have allowed the study of reactive intermediates, the composition of the OEC and the protein ligation of the metal centers. Unfortunately, while we now have a much better structural and mechanistic basis for PSII, we still are some way from the goal of a molecular mechanistic understanding of water oxidation. In extensive biomimetic efforts, numerous small molecule complexes have been synthesized in the hope of oxidizing water. Only a handful of these synthetic complexes have proved capable of oxidizing water to oxygen; however, some mechanistic information has been gained. Computational work has also begun to suggest possible pathways. This review will cover the chemistry of water oxidation by synthetic manganese and ruthenium complexes. Mention will be made both of biological systems and heterogeneous systems where appropriate, but these are not the focus of this review. A number of related reviews [15–22] have appeared.

2. Photosystem II and the oxygen-evolving complex

2.1 Structure

Photosystem II (PSII) is an enzyme found in the thylakoid membranes of oxygenic photosynthetic organisms. The protein complex forms as a dimer with a molecular weight of around 650 kDa. Although PSII is a large protein complex, much of its bulk is involved in harvesting and transferring photonic energy. The actual oxidation of water to oxygen is carried out at a cluster of metals referred to as the oxygen-evolving complex (OEC) [19]. Biochemical and biophysical experiments have long established that manganese is essential for photosynthetic water oxidation and EPR experiments have set the number of manganese atoms in the OEC at four [8,9,23]. In addition to the four manganese atoms, a calcium atom has been shown to be part of the OEC through EPR [10], EXAFS [24] and X-ray diffraction [1] experiments. Beyond the core structure of four manganese atoms and one calcium atom, a number of other components have been suggested for the OEC. These include chloride [25, 26] and bicarbonate [27–29] ions.

2.1.1 Crystal structure—Two recent crystal structures [1,2] have resolved the electron density of the OEC and proposed that it can be best fit by a trimanganese cluster with a single "dangler" manganese a slightly longer distance away (Figure 1A,B). There are some distinct differences between the two crystal structures that should be emphasized despite their general similarities. The 3.5 Å structure of Ferriera et al. [1] used X-ray anomalous difference maps at the Mn adsorption edge and at the wavelength where Ca^{2+} has an anomalous difference to determine what portion of the OEC electron density is due to either Mn or Ca^{2+}. Based on these data, the electron density at the OEC was modeled as a cubane-like Mn_3Ca cluster bridged by oxo atoms connected to the fourth Mn via one of the μ-oxo groups [1] (Figure 1A). Ferreira et al. [1] also tentatively assigned electron density at the proposed active site of the OEC to a bicarbonate ion (blue in Figure 1A). The model of the OEC from Loll et al. [2], based on a 3.0 Å structure, has substantial differences from the earlier 3.5 Å structure of Ferreira et al. [1]. Because the individual atoms are not resolved at the resolution of 3.0 Å the OEC was modeled without incorporating oxo bridges into the structure, and a slightly different arrangement of metal ions and ligands was modeled to fit the electron density (Figure 1B). In addition, no electron density was observed at the position corresponding to the bicarbonate ion modeled by Ferriera et al. [1].

2.1.2 Oriented EXAFS—While both of the crystal structures have offered new insight into the structure of the OEC, concerns that the OEC is being reduced during data collection has raised doubt as to the exact arrangement of the metal atoms [30]. To address this concern, oriented EXAFS experiments were carried out to determine the geometry of the OEC more accurately [3]. The lower X-ray exposure used for EXAFS experiments may avoid reduction of the manganese atoms in the OEC and allows for precise measurement of metal-metal distances. Unfortunately, the large number of metal atoms in the OEC make interpretation of the oriented EXAFS measurements difficult and the data have only been able to narrow the selection of possible geometries rather than determine a unique structure. Figure 1C shows one of the OEC structures proposed from the EXAFS measurements.

2.1.3 Calculations—In an effort to determine a more detailed structure of the OEC, quantum mechanical (QM) and molecular mechanics (MM) calculations were carried out that use the parameters of the 3.5 Å crystal structure and spectroscopic data [31–33]. Using a model including all residues within 15 Å of any of the OEC cluster atoms, a proposed structure for the OEC was calculated using (QM/MM) methods (Figure 1D). This structure is the only one to incorporate a chloride ion thought to be located in the OEC.

2.2 Mechanism

A number of proposals have been made for the mechanism of water oxidation at the OEC [19]. The most recent are based on the X-ray and QM/MM structures of the OEC [31,34–36]. Since the introduction of the S state cycle by Kok et al., it has been known that water is oxidized to oxygen through four distinct oxidation steps. The four oxidation steps, along with five proposed intermediates known as the S-states, are the basis of any PSII mechanism and are referred to as the Kok cycle [37] (Figure 2). While the Kok cycle defines the redox intermediates that are formed in the process of water oxidation, it provides no information at the molecular level. Following from the first modern "molecular"mechanism proposed by Brudvig and Crabtree in 1986 [38], a number of molecular mechanisms have been proposed over the years and these have been refined as new details of the active-site structure have become available. Mechanisms under current consideration will be outlined in this section and expanded upon where necessary in conjunction with relevant model systems.

2.2.1 Butterfly/double pivot Mechanism—The Dismukes and Christou groups have proposed a mechanism known as the butterfly or double pivot mechanism [39,40]. This involves an OEC structure with a cubane-like geometry composed of alternating metal and oxo units. In the double pivot mechanism, O_2 is evolved by O-O bond formation across a face of the cube and subsequent loss of O_2 freeing two of the manganese atoms to pivot outward and open the cube (Figure 3, top). This hypothesis is supported by gas phase experiments illustrating the formation of O_2 from Mn_4O_4 cuboidal complexes [40], as well as reduction of similar Mn_4O_4 complexes to form Mn_4O_2 and two water molecules [41,42]. The reduction reactions imply that the reverse oxidation reaction is possible. The mechanism is, however, disfavored by recent isotope exchange measurements, which show that μ-oxo groups in Mn model complexes exchange much more slowly than the substrates in the OEC [43].

2.2.2 2+2 mechanism—Babcock and coworkers originally proposed a popular mechanism referred to as the "2+2" mechanism [44] (Figure 4, bottom). The 2+2 mechanism assumes that the structure of the OEC is composed of two sets of manganese dimers in close proximity. It is proposed that each of the two dimers has water ligated in such a way that they, too, are in close proximity. The mechanism involves progressive oxidation of these two waters until a manganese oxo group is formed on one dimer and a hydroxide ion is coordinated to the other. The final oxidation invokes the removal of the last proton and formation of an O-O bond to form a peroxo species between the two dimers that quickly forms O_2. This mechanism has become less popular recently due to recent structural findings disfavoring the dimer-of-dimers structure that is the origin of the "2+2" name [1,2,23].

2.2.3 Nucleophilic attack of water/hydroxide on an electrophilic Mn=O—The remaining mechanistic proposals are largely related to one another and revolve around formation of a high-valent metal-oxo group that undergoes nucleophilic attack by a nearby water or hydroxide group (Figure 5, bottom). This family of mechanisms can be viewed as an adaptation of the 2+2 mechanism mentioned above that has been refashioned to reflect the most recent OEC structural model [45–49]. The result is a mechanism where a high-valent manganese-oxo is formed on the lone dangler manganese. This isolated manganese-oxo group is then proposed to react with a coordinated water or hydroxide [31,34]. The involvement of either a nucleophilic water or hydroxo is one area of contention in this mechanism. Both calcium and manganese have been proposed to be the coordination site of the second substrate water. Current X-ray crystallographic models for the OEC leave multiple coordination sites open on the nearby calcium and manganese atoms, leaving either option equally valid within the present limits of structural resolution [1,2]. Another area of contention in this mechanism centers on the nature of the high-valent manganese-oxo active species. Recently, it has been proposed that rather than an Mn(V)-oxo, which has not been spectroscopicaly observed [5,

50], the active species in the protein is actually a Mn(IV)-oxyl [35], a spin isomer of the Mn (V)-oxo having O radical character. With the oxyl form, Siegbahn [35] finds a 12.5 kcal/mol barrier for a terminal oxyl/bridging oxo coupling in the coordination sphere of Ca. He has also emphasized the importance of spin state considerations in formulating a viable mechanism. A detailed discussion of mechanisms involving manganese-oxo versus manganese-oxyl species can be found in reference [19]. Due to the difficulty in differentiating between a Mn(V)-oxo and a Mn(IV)-oxyl active species, we will refer to this species as a Mn(V)-oxo intermediate in this review.

3. Functional Models

In the decade since two previous reviews of the literature of OEC model complexes [18,20], significant advances have been made. The number of model complexes has expanded rapidly as groups have built upon the early examples. Ruthenium model chemistry was the first to achieve homogeneous water oxidation and has subsequently become the best characterized. More recently, functional manganese model complexes have been developed and have the added advantage of being more biologically relevant to the OEC. Finally, a great deal of work has been done to design heterogeneous systems that catalyze water oxidation.

3.1 Ruthenium chemistry

3.1.1 Oxo-bridged ruthenium dimers—The ruthenium dimer $[(bpy)_2(H_2O)Ru^{III}ORu^{III}(H_2O)(bpy)_2]^{+4}$ (where bpy is 2,2'-bipyridine) (**1**) is the first example of a homogeneous water oxidation catalyst [51,52]. Meyer et al. reported (**1**) in the early 1980's as a water-oxidation catalyst capable of a moderate number of turnovers (Table 1). Since that time, **1** has become one of the most studied water oxidation catalysts [53–57]. Even with 25 years of study, the mechanism by which **1** oxidizes water is still under active discussion [58–62].

Complex **1** has yielded water-oxidation catalysis by using a number of different primary oxidants including Co^{3+} [62], Ce^{IV} [52,63,64], and electrochemical oxidation [51,52,57,61, 65]. Using these one-electron oxidant systems has enabled the identification of every oxidation state of **1** between (III,III) and (V,V) [61]. The (V,V) oxidation state is often proposed to be the final one before oxygen is released [58]. Study of the spectroscopic features of various proposed intermediates of **1** along the catalytic cycle between the (III,III) and (V,V) oxidation states has been used to fit the data to a mechanistic model [61].

While a proposed intermediate for each of the oxidation states has been identified, many difficulties in identification of the catalytic reactions arise from conversion between oxidation states in catalytically active solutions and similar UV-vis spectra of the intermediate species [61]. As a result, there is no consensus on the exact mechanism of oxygen evolution by **1**. There are four main proposals, split into bimolecular and intramolecular pathways, as illustrated in Figure 6. All four mechanistic proposals are based on O-O bond formation by the bis oxo Ru (V,V) dimer that is the observed intermediate with the highest oxidation state [59].

The difficulties in monitoring **1** directly after the (V,V) state is reached has led to much kinetic information being garnered by observing the oxygen product rather than formation of the various Ru intermediates. Oxygen evolution in this, and most other systems, is monitored in one of two ways. First, the isotopic composition of the oxygen evolved is monitored by mass spectrometry. Second, the reaction kinetics and kinetic isotope effect are measured by observing the rate of oxygen evolution using a Clark-type oxygen electrode. Due to the slow exchange of ligands bound to Ru, the isotopic composition of evolved oxygen is very helpful in determining the mechanism of oxygen evolution [66]. Unfortunately, there is a conflict in the literature as to the relative isotopic composition of the evolved oxygen [59,67]. This may

be a function of instrumental differences. The most recent measurement determined that, when **1** was enriched with ^{18}O at the cis-aqua positions and further oxidized in unlabeled aqueous solution, the evolved oxygen contained mostly $^{18}O^{16}O$ and very little oxygen with a mass of 32 or 36 [59]. The earlier measurement found that the mixed-isotope product was less dominant [67]. The dominance of the mixed-isotope oxygen implies that oxygen is evolved through a mechanism involving a single oxo group bound to Ru and a solvent water molecule. This result would eliminate mechanisms A, B and D in Figure 6. In the earlier measurements where mixed-label oxygen was not such a dominant product, all four proposed mechanisms were still in play to some extent. In addition to the four mechanisms shown in Figure 6, a new and somewhat unorthodox mechanism has recently been put forth that involves the oxidation of one of the bipyridine ligands to a diol and subsequent reduction of this diol to release oxygen and regenerate the bipyridine ligand [59]. This fifth mechanism is supported by EPR measurements that suggest that the proposed (V,V) oxidation state may in fact be a (IV,V) species with a radical on one of the bipyridine ligands [68,69] and by observations of monomeric $Ru(bpy)_3$ complexes trapped in zeolite cages [70].

The most recent mechanistic proposal to include O-O bond formation has used DFT calculations to propose a mechanism involving a peroxo species by way of a ruthenium oxo radical that is very similar to mechanism C in Figure 6 [71]. This calculated mechanism is in agreement with the more recent mixed-label O_2 studies discussed above, as well as being analogous to the nucleophilic water mechanism for the OEC discussed above in section 2.2.3.

3.1.2 Ruthenium dimers bridged by amines—1 is the first of a series of ruthenium complexes that catalyze water oxidation. In addition to **1** and its related complexes [63], there is an emerging family of ruthenium dimer complexes bridged by amine-based ligands [72]. The $[Ru_2^{II}(\mu\text{-OAc})(bpp)(tpy)_2]^{2+}$ (**2**) dimer [73] (where bpp = 3,5-di(2-pyridyl)pyrazole and tpy = 2,2':6',2"-terpyridine) (Figure 7) is an example of the new class of complexes with amine-based ligands. Complex **2** has been shown to oxidize water at both a faster rate and with higher turnovers than **1** (Table 1). **2** catalyzes oxygen evolution at a rate of 1.4×10^{-2} s^{-1} with a turnover number of 18.6 when Ce^{IV} is used as an oxidant. While the increase in rate requires more investigation, the increase in turnover number is at least partially credited to the removal of the oxo bridge present in **1** [63,64,73]. The oxo bridge has been proposed to be a weak point in the structure of **1**, facilitating decomposition through disproportionation to a high-valent Ru-oxo monomer and a low-valent Ru-bipyridine complex. The increased turnover number observed in other examples of amine-based ruthenium dimers such as $[(bnp)(4\text{-methylpyridine})_2Ru(\mu\text{-Cl})Ru(4\text{-methylpyridine})_2\}^{3+}$ (**3**), where bnp = 3,6-bis-[6'-(1",8"-naphthyrid-2"-yl)-pyrid-2'-yl]pyridazine, supports the hypothesis (Table 1).

3.1.3 Ruthenium monomers—An amine-based ligand may also stabilize the rare example of a mononuclear water-oxidation catalyst (**4**) [74], shown in Figure 7. **4** has been shown to evolve oxygen at a rate of 3.5×10^{-4} s^{-1} with 580 turnovers using Ce^{IV} as an oxidant (Table 1). Complex **4** and related molecules appear to be mononuclear under catalytic conditions and show good oxygen evolving activity, but the possibility of dimerization is still present and past studies have shown that water oxidation with less than a dimeric complex is unfavorable [75].

3.1.4 $[Ru_2^{II}(OH)_2(3,6\text{-}t\text{-}Bu_2quinone)_2(btpyan)]^{2+}$—Finally, $[Ru_2^{II}(OH)_2(3,6\text{-}t\text{-}Bu_2quinone)_2(btpyan)]^{2+}$ (**5**) (btpyan = 1,8-bis{(2,2':6'2")-terpyridyl}anthracene) has been found to be an active water-oxidation catalyst [76–78]. Complex **5** has been found to catalyze the electrochemical oxidation of water to oxygen. However, unlike the previous complexes, no oxidation is observed in the presence of a chemical oxidant. While modest activity is observed when the complex is in solution, a turnover number of 2400 is observed when the complex is attached to the indium tin oxide electrode surface, a 100-fold increase over the

homogeneous system. The turnover number for **5** on the electrode surface can be improved to over 33000 turnovers through the addition of base to absorb the protons built up during the reaction.

3.2 Manganese chemistry

While the stability of ruthenium ligand bonds has allowed many stable water-oxidation catalysts to be developed and intermediate oxidation states to be characterized, to truly mimic the oxygen-evolving center of PSII, a model complex using manganese is needed. The challenge in switching from a ruthenium system to a manganese system is largely one of ligand lability [43]. Studies on the decomposition of **1** indicate that the instability of the complex is linked to complications involving the bridging oxo unit [63,64,73]. However, the terminal ligands of Ru complexes are very stably bound. Indeed, one disadvantage of **1** as a water-oxidation catalyst is that it can bind anions very tightly, leading to deactivation of the complex by ligation of anions [58].

On the other hand, the lability of the ligands of non-porphyrin manganese complexes is greatly increased over that of similar ruthenium complexes [43]. This is an advantage for rapid catalytic turnover of Mn complexes, which can rapidly exchange the substrates and products bound to Mn. However, ligand lability of Mn complexes can lead to instability of the catalyst under catalytic conditions, although Nature has overcome this problem of ligand lability by encapsulating the Mn ions in the OEC within the proteins of PSII. While instability is an issue for manganese model complexes, a number of successes have been reported [40,79–83]. In this section, the manganese-based synthetic water-oxidation catalysts will be examined and their proposed mechanisms compared to the mechanisms proposed for the OEC.

3.2.1 Bis-porphyrin model—The bis-porphyrin model compound reported by Naruta et al. [80,84] (Figure 4, top) uses the known stability of manganese porphyrin complexes to circumvent the ligand lability issues of Mn mentioned above. By coupling two stable manganese-oxo-forming units together, a bis Mn(V)=O intermediate can be isolated after addition of m-chloroperbenzoic acid. Isolation of the bis-Mn(V)-oxo intermediate is the key to this complex because it suggests that the common radical-based chemistry associated with most organic peroxides and peracids is not involved. After formation of the bis-Mn(V)=O intermediate, oxygen can be evolved in stoichiometric quantities upon the addition of an excess of triflic acid. Addition of acid protonates the hydroxo ligand trans to the Mn=O unit and helps to destabilize one or both of the oxo units leading to formation of an oxygen-oxygen bond. While this complex is only a single turnover 'catalyst' it is important in that it allows examination of a model complex that closely mimics the mechanism for oxygen evolution proposed by Hoganson and Babcock [44], shown in Figure 4 (bottom). The two mechanisms are very similar in that they propose the formation of a high-valent manganese-oxo group in close proximity to a manganese-bound oxo or hydroxo that can act as a nucleophile to attack the electrophilic oxo group and create an O-O bond. The main difference lies in the last step before formation of the O-O bond. The Naruta et al. [80] complex is oxidized by the full four electrons to form a stable bis-oxo species which is then destabilized to initiate O-O bond formation, while the Hoganson and Babcock mechanism [44] proposes the formation of the O-O bond simultaneously with the removal of the fourth electron and proton. This difference is minor if you consider that the bis-oxo species isolated in the Naruta et al. system [80] can be viewed as an intermediate species formed during the final oxidation step in the Hoganson and Babcock mechanism [44].

3.2.2 Cubane model—A second example of an oxygen-evolving molecule that closely mimics a proposed OEC mechanism is the $L_6Mn_4O_4$ (L = diphenylphosphinate anion ($Ph_2PO_2^-$)) cubane-like complex developed by Dismukes and coworkers [40,85,86]. This

cubane-like complex has been shown to release one equivalent of O_2 from each tetramanganese cluster under the gas phase conditions of a laser desorption ionization mass spectrometry (LDI-MS) system when pulsed with 355 nm light. The solid cubane-like complex is ionized by a laser pulse and the mass spectrometer detects both the starting material and the product which is two oxygen atoms lighter. To determine that the product of this reaction was oxygen and not some unseen oxidation product, the cubane-like complex was subjected to pulsed laser radiation similar to the LDI-MS experiment, but in this case, the gas evolved was sampled by a mass spectrometer sensitive to lower masses. It has been proposed that the mechanism of O_2 evolution involves the formation of an O-O bond across two corners of the cubane complex as shown in Figure 3 (bottom). This is similar to the 'double pivot' mechanism proposed for oxygen evolution [39] from the OEC shown in Figure 3 (top).

3.2.3 $[Mn(3,5, Cl\text{-}salen)(H_2O)_2]_2$—A third single-turnover oxygen-evolution system is the $[Mn(3,5\text{-}Cl\text{-}salen)(H_2O)_2]_2$ complex (where 3,5-Cl-salen = N,N'3,5-dichlorobis (salicylidene)-1,2-diaminoethane) and the related binucleating complex [81,87–89]. In this system, O_2 is proposed to be evolved through a mechanism involving the photolytic oxidation of two bridging water molecules coupled to the reduction of *p*-benzoquinone to the catechol (Figure 8). This complex represents a rare example of homogeneous photolytic oxidation of water to oxygen.

3.2.4 $[Mn^{II}_2(mcbpen)_2(H_2O)_2]^{2+}$—Only two multi-turnover Mn-based homogeneous catalysts have been reported: $[Mn^{II}_2(mcbpen)_2(H_2O)_2]^{2+}$ (**6**) and $[(tpy)(H_2O)Mn(O)_2Mn(H_2O)(tpy)]^{3+}$ (**7**). We will discuss each of these in turn.

The most recent example of a homogeneous manganese catalyst capable of oxidizing water to oxygen $[Mn^{II}_2(mcbpen)_2(H_2O)_2]^{2+}$ (mcbpen = N-methyl-N'-carboxymethyl-N,N'-bis(2-pyridylmethyl)ethane-1,2-diamine) was developed by McKenzie et al. [82]. This complex is capable of carrying out the four-electron oxidation of water by conversion of the Mn(II/II) and Mn(IV,IV) oxidation states through a proposed mechanistic pathway shown in Figure 9. The oxidation is accomplished with ca. 10–20 turnovers using *tert*-butylhydrogenperoxide (TBHP) and with less efficiency using cerium(IV) as an oxidant (Table 1). In this system, the use of TBHP is an interesting choice of oxidant due to its tendency toward radical chemistry [90, 91]. The authors address the concerns of water oxidation from radical versus oxo-based chemistry by repeating their water-oxidation experiments using ceric ammonium nitrate as the oxidant. Oxidation by Ce(IV) is a mechanistically reliable oxidation in the sense that it can only transfer one electron per Ce(IV) and does not involve the donation of an oxygen atom in the process of oxidation. The Ce(IV) oxidation experiments are somewhat problematic in that the oxidation of water using Ce(IV) yields a much smaller quantity of oxygen when compared to TBHP but the oxygen evolved from H_2O^{18} was composed entirely of mixed $^{18}O^{16}O$ oxygen. The authors suggest that the unlabeled oxygen could come from the nitrate counter ion of the oxidant. The inclusion of unlabeled oxygen, possibly from a nitrate, is highly unusual and further mechanistic work is needed to clarify the water-oxidation chemistry of the McKenzie et al. system. In addition, mechanisms involving the coupling of μ-oxo's, such as the double pivot mechanism (Figure 3) and the McKenzie et al. mechanism (Figure 9), are disfavored in the OEC based on recent measurements of the μ-oxo exchange rates [43,92].

3.2.5 $[(tpy)(H_2O)Mn(O)_2Mn(H_2O)(tpy)]^{3+}$—The first reported multi-turnover Mn-based homogeneous water-oxidation catalyst is $[(tpy)(H_2O)Mn(O)_2Mn(H_2O)(tpy)]^{3+}$(**7**) (where tpy = 2,2':6',2"-terpyridine) (Figure 10) developed by Brudvig and Crabtree [83]. **7** is most commonly isolated in the Mn(III,IV) oxidation state and is proposed to carry out the four-electron oxidation of water by passing through the Mn(II,III) to Mn(IV,V) oxidation states [93, 94]. To date, this complex has only been able to oxidize water catalytically using two-electron oxygen-atom donor oxidants such as HSO_5^- (oxone) or ClO^- through a mechanism

shown in Figure 5 (top). The mechanism shown in Figure 5 (top) is the result of isotope labeling studies which show that under high concentrations of oxidant the oxygen produced contains minimal ^{18}O label from the solvent while at lower concentrations of oxidant a significant fraction of the product contains a single oxygen from the solvent and some of the evolved O_2 contains two oxygen from the solvent [93]. The fact that only oxygen-atom donor oxidants are functional has been a concern for this system [95], but recent results have shown that the catalyst is capable of oxygen evolution using Ce(IV) as an oxidant. Catalytic turnover is not attained when Ce(IV) is used as the oxidant due to the low pH required for use of Ce(IV) as an oxidant which causes deactivation of the catalyst [96]. In contrast to the single-turnover oxygen evolution by the homogeneous system using Ce(IV), **7** has been shown to evolve oxygen catalytically using Ce(IV) when it is supported on a clay mineral [97, 98]. The dramatic improvement of **7** in heterogeneous versus homogenous systems with Ce(IV) is proposed to be the result of the stabilizing clay environment which prevents the dimer from dissociating into monomers. At low pH, the μ-oxo bridges of **7** are protonated in low-valent states of the complex weakening a ligand that is already a source of concern, as stated above in the Ru systems.

Similarly to the Ru-based complex **1**, the oxygen-evolution mechanism proposed for **7** involves a high-valent Mn=O species which undergoes nucleophilic attack by a water or hydroxide [19,34]. Although both complexes **1** and **7** model the same proposed mechanism for oxygen evolution at the OEC, **7** has a marked advantage in that it consists of the biologically active metal. Recent studies of **7** have revealed ligand and electron exchange rates that can be directly applied to our mechanistic understanding of the OEC [99]. One area of contention in the nucleophilic water mechanism for the OEC that is modeled by both **1** and **7** is the location of the nucleophilic water. In the Messinger mechanism [34], the nucleophilic oxygen is a μ-oxo group, while in the mechanism proposed by McEvoy et al. [31] the nucleophilic water is bound to the Ca^{2+} ion. Due to similarities in oxidation state and structure to OEC in the S_2 state, complex **7** can be used as a model for μ-oxo exchange. Comparison of the μ-oxo exchange rate in **7** to the exchange rate of the substrate waters in the OEC measured by Wydrzynski and coworkers [48,100,101] suggests that the nucleophilic oxygen does not originate from one of bridging oxo groups [43,92].

4. Heterogeneous systems

In addition to the complexes listed above, a number of less-well-defined catalysts have been found to evolve oxygen under certain conditions. Oxides of metals such as iridium, ruthenium, and manganese, in addition to platinum black, are known to evolve small amounts of oxygen in the presence of strong oxidants such as Ce(IV) or oxone [16,102,103]. Permanganate solutions have been known to evolve oxygen when dissolved in water, with MnO_4^- acting as a catalytic oxidant [104]. Ruthenium complexes using ammonia as a ligand, such as $[(NH_3)_5RuORu(NH_3)_4ORu(NH_3)_5]^{6+}$, also known as ruthenium red, have also been shown to have very high activity for oxygen evolution, especially when stabilized as a heterogeneous system [105–107]. As shown in Table 1, complexes such as Ru red have oxygen-evolution characteristics comparable to the more well-defined model systems in solution and these characteristics have been found to be considerably improved upon isolation of the catalyst in polymers such as Nafion [55]. Due to the heterogeneous nature of these systems, they will not be covered in detail. More information can be found in the following reviews [16,20].

5. Conclusions

Photosystem II is a very challenging protein to study by biophysical methods. Recent advances by the biophysical community have allowed for greater insights into the active site of the protein than ever before, but we are still far from the goal of a detailed understanding of the molecular

mechanism of water oxidation by the OEC. To elucidate the details of the OEC reaction mechanism, bioinorganic chemists have made many new complexes to mimic the proposed biological mechanisms. As described above, there has been moderate success in creating and studying new biological mimics. Work on small molecules has clarified many issues relevant to the OEC such as the necessity of multiple metals and the importance of proton transfer. Functional model systems are still very much less active than the OEC, but current mechanistic models show activity very analogous to mechanisms proposed for the OEC. As shown in Table 1, the activity of the synthetic systems can best be described as modest. However, the study of model complexes that are capable of generating high-valent Mn-oxo groups that are then nucleophilicly attacked by a substrate water will greatly improve our understanding of the natural water-oxidation mechanism. The model systems discussed in this review have made the challenges of water oxidation clearer and more probing experiments are being developed.

Acknowledgments

Funding from National Institutes of Health grant GM32715 and National Science Foundation grant CHE-0614403 is gratefully acknowledged.

References

1. Ferreira KN, Iverson TM, Maghlaoui K, Barber J, Iwata S. Science 2004;303:1831–1838. [PubMed: 14764885]
2. Loll B, Kern J, Saenger W, Zouni A, Biesadka J. Nature 2005;438:1040–1044. [PubMed: 16355230]
3. Yano J, Kern J, Sauer K, Latimer MJ, Pushkar Y, Biesiadka J, Loll B, Saenger W, Messinger J, Zouni A, Yachandra VK. Science 2006;314:821–825. [PubMed: 17082458]
4. Haumann M, Müller C, Liebisch P, Iuzzolino L, Dittmer J, Grabolle M, Neisius T, Meyer-Klaucke W, Dau H. Biochemistry 2005;44:1894–1908. [PubMed: 15697215]
5. Haumann M, Liebisch P, Müller C, Barra M, Grabolle M, Dau H. Science 2005;310:1019–1021. [PubMed: 16284178]
6. Robblee JH, Cinco RM, Yachandra VK. Biochim.Biophys. Acta 2001;1503:7–23. [PubMed: 11115621]
7. Yachandra VK, Sauer K, Klein MP. Chem.Rev 1996;96:2927–2950. [PubMed: 11848846]
8. Dismukes GC, Siderer Y. Proc.Natl. Acad.Sci 1981;78:274–278. [PubMed: 16592949]
9. de Paula JC, Beck WF, Brudvig GW. J. Am. Chem. Soc 1986;108:4002–4009.
10. Kim SH, Gregor W, Peloquin JM, Brynda M, Britt RD. J. Am. Chem. Soc 2004;126:7228–7237. [PubMed: 15186160]
11. Koulougliotis D, Shen J-R, Ioannidis N, Petrouleas V. Biochemistry 2003;42:3045–3053. [PubMed: 12627971]
12. Miller A-F, Brudvig GW. Biochim. Biophys. Acta 1991;1056:1–18. [PubMed: 1845842]
13. Debus RJ, Strickler MA, Walder LM, Hillier W. Biochemistry 2005;44:1367–1374. [PubMed: 15683222]
14. Noguchi, T.; Berthomieu, C. Photosystem II The Light-Driven Water: Plastoquinone Oxidoreductase. Wydrzynski, TJ.; Satoh, K., editors. Dordrecht, The Netherlands: Springer; 2005. p. 367-387.
15. Meyer TJ. Acc. Chem. Res 1989;22:163–170.
16. Yagi M, Kaneko M. Chem. Rev 2001;101:21–35. [PubMed: 11712192]
17. Mukhopadhyay S, Mandal SK, Bhaduri S, Armstrong WH. Chem.Rev 2004;104:3981–4026. [PubMed: 15352784]
18. Manchanda R, Brudvig GW, Crabtree RH. Coord. Chem. Rev 1995;144:1–38.
19. McEvoy JP, Brudvig GW. Chem. Rev 2006;106:4455–4483. [PubMed: 17091926]
20. Rüttinger W, Dismukes GC. Chem. Rev 1997;97:1–23. [PubMed: 11848863]
21. Tommos C, Babcock GT. Acc. Chem. Res 1998;31:18–25.
22. Diner BA, Rappaport F. Annu. Rev. Plant Biol 2002;53:551–580. [PubMed: 12221988]

23. Peloquin JM, Campbell KA, Randall DW, Evanchik MA, Pecoraro VL, Armstrong WH, Britt RD. J. Am. Chem. Soc 2000;122:10926–10942.
24. Cinco RM, Holman KLM, Robblee JH, Yano J, Pizarro SA, Bellacchio E, Sauer K, Yachandra VK. Biochemistry 2002;41:12928–12933. [PubMed: 12390018]
25. Pizarro SA, Visser H, Cinco RM, Robblee JH, Pal S, Mukhopadhyay S, Mok HJ, Sauer K, Wieghardt K, Armstrong WH, Yachandra VK. J. Biol. Inorg. Chem 2004;9:247–255. [PubMed: 14758524]
26. Homann PH. Photosynth. Res 2002;73:169–175. [PubMed: 16245119]
27. Siegbahn PEM, Lundberg M. J. Inorg. Biochem 2006;100:1035–1040. [PubMed: 16584780]
28. Baranov SV, Ananyev GM, Klimov VV, Dismukes GC. Biochemistry 2000;39:6060–6065. [PubMed: 10821678]
29. Baranov SV, Tyryshkin AM, Katz D, Dismukes GC, Ananyev GM, Klimov VV. Biochemistry 2004;43:2070–2079. [PubMed: 14967047]
30. Yano J, Kern J, Irrgang K-D, Latimer MJ, Bergmann U, Glatzel P, Pushkar Y, Biesiadka J, Loll B, Sauer K, Messinger J, Zouni A, Yachandra VK. Proc. Natl. Acad. Sci 2005;102:12047–12052. [PubMed: 16103362]
31. McEvoy JP, Gascon JA, Batista VS, Brudvig GW. Photochem. Photobiol. Sci 2005;4:940–949. [PubMed: 16307106]
32. Sproviero EM, Gascon JA, McEvoy JP, Brudvig GW, Batista VS. J. Inorg. Biochem 2006;100:786–800. [PubMed: 16510187]
33. Sproviero EM, Gascon JA, McEvoy JP, Brudvig GW, Batista VS. J. Chem. Theory. Comput 2006;2:1119–1134.
34. Messinger J. Phys. Chem. Chem. Phys 2004;6:4764–4771.
35. Siegbahn PEM. Chem. Eur. J 2006;12:9217–9227.
36. McEvoy JP, Brudvig GW. Phys. Chem. Chem. Phys 2004;6:4754–4763.
37. Kok B, Forbush B, McGloin M. Photochem. Photobiol 1970;11:457. [PubMed: 5456273]
38. Brudvig GW, Crabtree RH. Proc. Natl. Acad. Sci 1986;83:4586–4588. [PubMed: 3460059]
39. Vincent JB, Christou G. Inorg. Chim. Acta 1987;136:L41–L43.
40. Ruettinger W, Yagi M, Wolf K, Bernasek S, Dismukes GC. J. Am. Chem. Soc 2000;122:10353–10357.
41. Carrell TG, Bourles E, Lin M, Dismukes GC. Inorg. Chem 2003;42:2849–2858. [PubMed: 12716176]
42. Maneiro M, Ruettinger WF, Bourles E, McLendon GL, Dismukes GC. Proc. Natl. Acad. Sci 2003;100:3707–3712. [PubMed: 12644708]
43. Tagore R, Chen H, Crabtree RH, Brudvig GW. J. Am. Chem. Soc 2006;128:9457–9465. [PubMed: 16848483]
44. Hoganson CW, Babcock GT. Science 1997;277:1953–1956. [PubMed: 9302282]
45. Limburg J, Szalai VA, Brudvig GW. J. Chem. Soc. Dalton Trans 1999:1353–1361.
46. Vrettos JS, Limburg J, Brudvig GW. Biochim. Biophys. Acta 2001;1503:229–245. [PubMed: 11115636]
47. Pecoraro VL, Baldwin MJ, Caudle MT, Hsieh W-Y, Law NA. Pure Appl. Chem 1998;70:925–929.
48. Messinger J, Badger M, Wydrzynski T. Proc. Natl. Acad. Sci 1995;92:3209–3213. [PubMed: 11607525]
49. Dau H, Iuzzolino L, Dittmer J. Biochim. Biophys. Acta 2001;1503:24–39. [PubMed: 11115622]
50. Weng T-C, Hsieh W-Y, Uffelman ES, Gordon-Wylie SW, Collins TJ, Pecoraro VL, Penner-Hahn JE. J. Am. Chem. Soc 2004;126:8070–8071. [PubMed: 15225020]
51. Gersten SW, Samuels GJ, Meyer TJ. J. Am. Chem. Soc 1982;104:4029–4030.
52. Gilbert JA, Eggleston DS, Wyatt R, Murphy J, Geselowitz DA, Gersten SW, Hodgson DJ, Meyer TJ. J. Am. Chem. Soc 1985;107:3855–3864.
53. Rotzinger FP, Munavalli S, Comte P, Hurst JK, Gratzel M, Pern F-J, Frank AJ. J. Am. Chem. Soc 1987;109:6619–6626.
54. Raven SJ, Meyer TJ. Inorg. Chem 1988;27:4478–4483.
55. Nagoshi K, Yamashita S, Yagi M, Kaneko M. J. Mol. Cat. A 1999;144:71–76.

56. Okamoto K, Miyawaki J, Nagai K, Matumura D, Nojima A, Yokoyama T, Kondoh H, Ohta T. Inorg. Chem 2003;42:8682–8689. [PubMed: 14686845]
57. Vining WJ, Meyer TJ. Inorg. Chem 1986;25:2023–2033.
58. Binstead RA, Chronister CW, Ni J, Hartshorn CM, Meyer TJ. J. Am. Chem. Soc 2000;122:8464–8473.
59. Yamada H, Siems WF, Koike T, Hurst JK. J. Am. Chem. Soc 2004;126:9786–9795. [PubMed: 15291582]
60. Bartolotti LJ, Pedersen LG, Meyer TJ. Int. J. Quantum Chem 2001;83:143–149.
61. Chronister CW, Binstead RA, Ni J, Meyer TJ. Inorg. Chem 1997;36:3814–3815.
62. Hurst JK, Zhou J, Lei Y. Inorg. Chem 1992;31:1010–1017.
63. Lebeau EL, Adeyemi SA, Meyer TJ. Inorg. Chem 1998;37:6476–6484. [PubMed: 11670768]
64. Lebeau EL, Meyer TJ. Inorg. Chem 1999;38:2174–2181. [PubMed: 11671003]
65. Liu F, Cardolaccia T, Hornstein BJ, Schoonover JR, Meyer TJ. J. Am. Chem. Soc 2007;129:2446–2447. [PubMed: 17284036]
66. Yamada H, Koike T, Hurst JK. J. Am. Chem. Soc 2001;123:12775–12780. [PubMed: 11749534]
67. Geselowitz D, Meyer TJ. Inorg. Chem 1990;29:3894.
68. Yamada H, Hurst JK. J. Am. Chem. Soc 2000;122:5303–5311.
69. Lei Y, Hurst JK. Inorg. Chem 1994;33:4460–4467.
70. Ledney M, Dutta PK. J. Am. Chem. Soc 1995;117:7687–7695.
71. Yang X, Baik M-H. J. Am. Chem. Soc 2006;128:7476–7485. [PubMed: 16756301]
72. Rodriquez M, Romero I, Sens C, Llobet A. J. Mol. Cat 2006;A251:215–220.
73. Sens C, Romero I, Rodriguez M, Llobet A, Parela T, Benet-Buchholz J. J. Am. Chem. Soc 2004;126:7798–7799. [PubMed: 15212526]
74. Zong R, Thummel RP. J. Am. Chem. Soc 2005;127:12802–12803. [PubMed: 16159265]
75. Collin JP, Sauvage JP. Inorg. Chem 1986;25:135–141.
76. Wada T, Tsuge K, Tanaka K. Inorg. Chem 2001;40:329–337. [PubMed: 11170540]
77. Wada T, Tanaka K. Eur. J. Inorg. Chem 2005:3832–3839.
78. Wada T, Tsuge K, Tanaka K. Angew. Chem. Int. Ed 2000;39:1479–1482.
79. Chen H, Tagore R, Das S, Incarvito C, Faller JW, Crabtree RH, Brudvig GW. Inorg. Chem 2005;44:7661–7670. [PubMed: 16212393]
80. Shimazaki Y, Nagano T, Takesue H, Ye B-H, Tani F, Naruta Y. Angew. Chem. Int. Ed 2004;43:98–100.
81. Ashmawy FM, McAuliffe CA, Parish RV, Tames J. J. Chem. Soc. Dalton Trans 1985:1391–1397.
82. Pulsen AK, Rompel A, McKenzie CJ. Angew. Chem. Int. Ed 2005;44:6916–6920.
83. Limburg J, Vrettos JS, Liable-Sands LM, Rheingold AL, Crabtree RH, Brudvig GW. Science 1999;283:524–527.
84. Naruta Y, Sasayama M-a, Sasaki T. Angew. Chem. Int. Ed 1994;33:1839–1840.
85. Wu J-Z, Sillitto E, Yap GPA, Sheats J, Dismukes GC. Inorg. Chem 2004;43:5795–5797. [PubMed: 15360226]
86. Wu J-Z, Angelis FD, Carrell TG, Yap GPA, Sheats J, Car R, Dismukes GC. Inorg. Chem 2006;45:189–195. [PubMed: 16390055]
87. Garcia-Deibe A, Sousa A, Bermejo MR, Rory PPM, McAuliffe CA, Pritchard RG, Helliwell M. J. Chem. Soc., Chem. Commun 1991:728–729.
88. Aurangzeb N, Hulme CE, McAuliffe CA, Pritchard RG, Watkinson M, Bermejo MR, Garcia-Deibe A, Rey M, Sanmartin J, Sousa A. J. Chem. Soc., Chem. Commun 1994:1153–1155.
89. Watkinson M, Whiting A, McAuliffe CA. J. Chem. Soc., Chem. Commun 1994:2141–2142.
90. Caudle MT, Pecoraro VL. J. Am. Chem. Soc 1997;119:3415–3416.
91. Wessel J, Crabtree RH. J. Mol. Cat 1996;A113:13–22.
92. Tagore R, Crabtree RH, Brudvig GW. Inorg. Chem 2007;46:2193–2203. [PubMed: 17295472]
93. Limburg J, Vrettos JS, Chen H, Paula JCD, Crabtree RH, Brudvig GW. J. Am. Chem. Soc 2001;123:423–430. [PubMed: 11456544]

94. Chen H, Tagore R, Olack G, Vrettos JS, Weng T-C, Penner-Hahn J, Crabtree RH, Brudvig GW. Inorg. Chem 2007;46:34–43. [PubMed: 17198410]

95. Baffert C, Romain S, Richardot A, Lepretre J-C, Lefebvre B, Deronzier A, Collomb M-N. J. Am. Chem. Soc 2005;127:13694–13704. [PubMed: 16190735]

96. Tagore R, Chen H, Zhang H, Crabtree RH, Brudvig GW. Inorg. Chim. Acta 2007;360:2983–2989.

97. Yagi M, Narita K. J. Am. Chem. Soc 2004;126:8084–8085. [PubMed: 15225027]

98. Narita K, Kuwabara T, Sone K, Shimizu K-i, Yagi M. J. Phys. Chem. B 2006;110:23107–23114. [PubMed: 17107151]

99. Tagore R, Crabtree RH, Brudvig GW. Inorg. Chem. 2007 Submitted.

100. Hendry G, Wydrzynski T. Biochemistry 2002;41:13328–13334. [PubMed: 12403635]

101. Hendry G, Wydrzynski T. Biochemistry 2003;42:6209–6217. [PubMed: 12755624]

102. Howelles AR, Sankarraj A, Shannon C. J. Am. Chem. Soc 2004;126:12258–12259. [PubMed: 15453746]

103. Ebina Y, Sakai N, Sasaki T. J. Phys. Chem. B 2005;109:17212–17216. [PubMed: 16853196]

104. Shafirovich VY, Khannonov NK, Shilov AE. J. Inorg. Biochem 1981;15:113–129.

105. Yagi M, Tokita S, Nagoshi K, Ogino I, Kaneko M. J. Chem. Soc. Faraday Trans 1996;92:2457–2461.

106. Yagi M, Sukegawa N, Kaneko M. J. Phys. Chem. B 2000;104:4111–4114.

107. Kinoshita K, Yagi M, Kaneko M. Macromolecules 1998;31:6042–6045.

108. Chow, WS.; Aro, E-M. Photosystem II the Light-Driven Water:Plastoquinone Oxoreductase. Wydrzynski, TJ.; Satoh, K., editors. Dordrecht, The Netherlands: Springer; 2005. p. 627-648.

109. Berthold D, Babcock GT, Yocum C. FEBS Letters 1981;134:231–234.

110. Limburg, J. Ph.D. Thesis. New Haven, CT: Department of Chemistry, Yale University; 1999.

111. Limburg J, Brudvig GW, Crabtree RH. J. Am. Chem. Soc 1997;119:2761–2762.

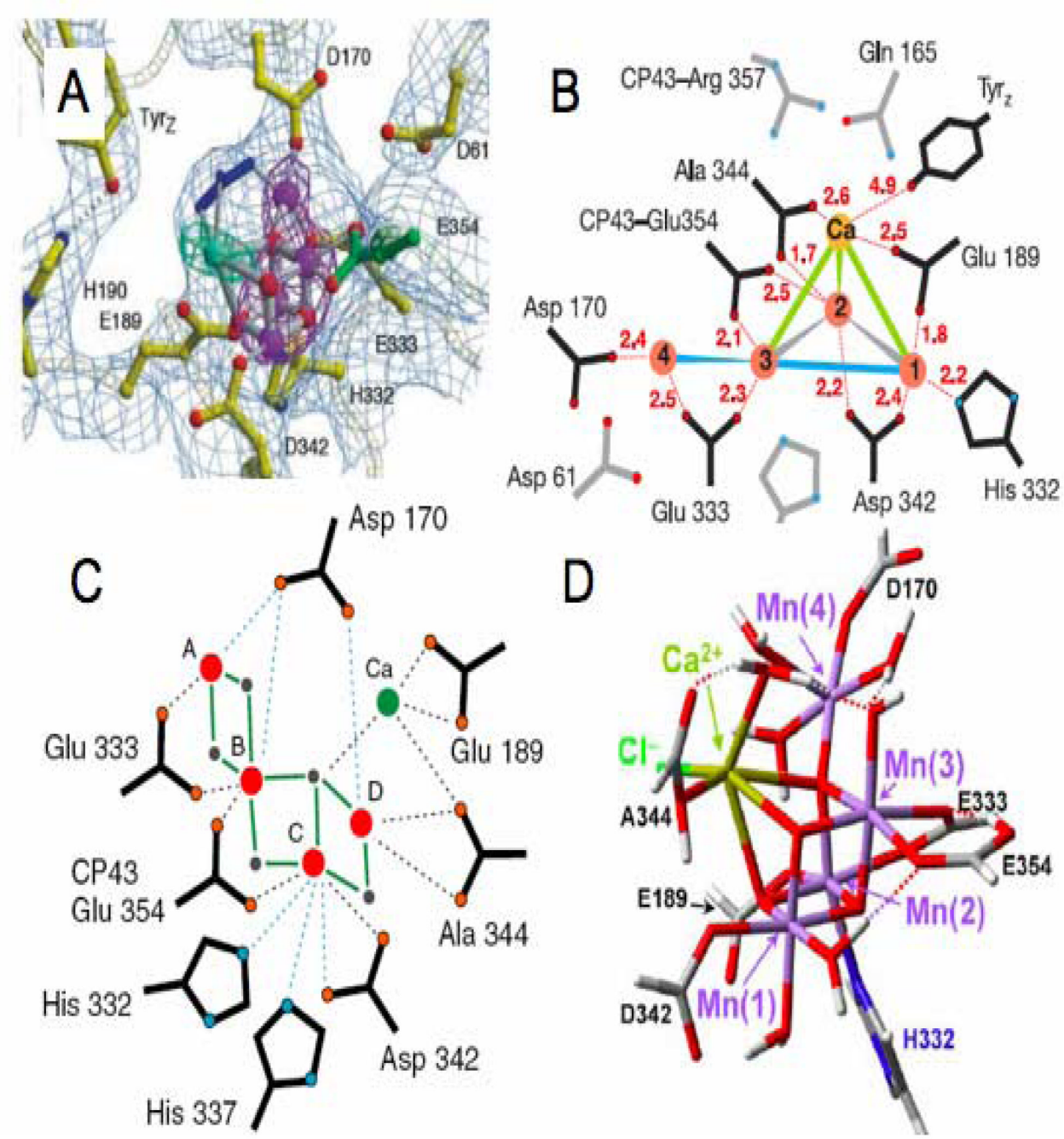

Figure 1.

Four proposed structures for the OEC of PSII. A) 3.5 Å crystal structure model of the OEC with anomalous diffraction electron densities of manganese and calcium in purple and cyan, respectively (figure was reproduced from ref. [1], with permission of the copyright holders). B) 3.0 Å crystal structure model of the OEC (figure was reproduced from ref. [2], with permission of the copyright holders). C) One of three proposed structures for the OEC determined by oriented EXAFS spectroscopy (figure was reproduced from ref. [3], with permission of the copyright holders). D) OEC structure calculated using QM/MM methods and basic structural parameters from the 3.5 Å structure (figure was reproduced from ref. [32], with permission of the copyright holders).

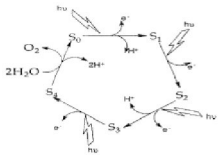

Figure 2.
Schematic diagram of Kok's S-state cycle showing four oxidations necessary for water oxidation (figure was reproduced from ref. [18], with permission of the copyright holders).

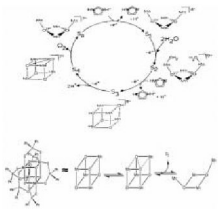

Figure 3.

Top: The proposed mechanism for water oxidation by the OEC known as the “double pivot”or “butterfly” mechanism. This mechanism is based on a cubane-type structure for the OEC (figure was reproduced from ref. [39], with permission of the copyright holders). Bottom: Schematic representation of the structure of the cubane-like complex synthesized by Dismukes et al. as well as its proposed mechanism of oxygen evolution (Figure was reproduced from ref. [40], with permission of the copyright holders).

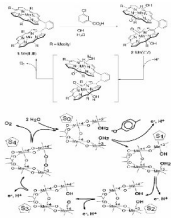

Figure 4.
Top: bis-porphyrin functional model for oxygen evolution (figure was reproduced from ref. [80], with permission of the copyright holders). Bottom: a proposed mechanism for biological oxygen evolution that closely resembles the proposed reactions of the bis-porphyrin complex (figure was reproduced from ref. [44], with permission of the copyright holders).

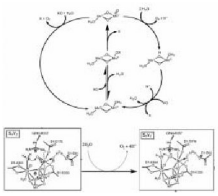

Figure 5.
Top: schematic diagram of the proposed mechanism of water oxidation by complex **7** (figure was reproduced from ref. [93], with permission of the copyright holders). Bottom: schematic representation of the proposed O-O bond forming step in the OEC based on the nucleophilic water mechanism (figure was reproduced from ref. [19], with permission of the copyright holders).

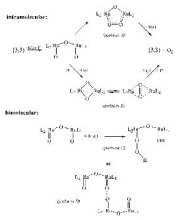

Figure 6.
Schematic diagram showing the four main pathways proposed for water oxidation by **1** (figure was reproduced from ref. [59], with permission of the copyright holders).

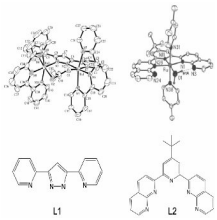

Figure 7.

ORTEP diagrams of $[Ru_2^{II}(\mu\text{-OAc})(bpp)(trpy)_2]^{2+}$ (**2**) (top left) (figure was reproduced from ref. [73], with permission of the copyright holders) and a catalytic ruthenium monomer system **4** (top right) (figure was reproduced from ref. [74], with permission of the copyright holders). Chemdraw diagrams of the bridging ligand in complex **2** (L1) as well as the multi-dentate ligand from complex **4** (L2) are shown (bottom).

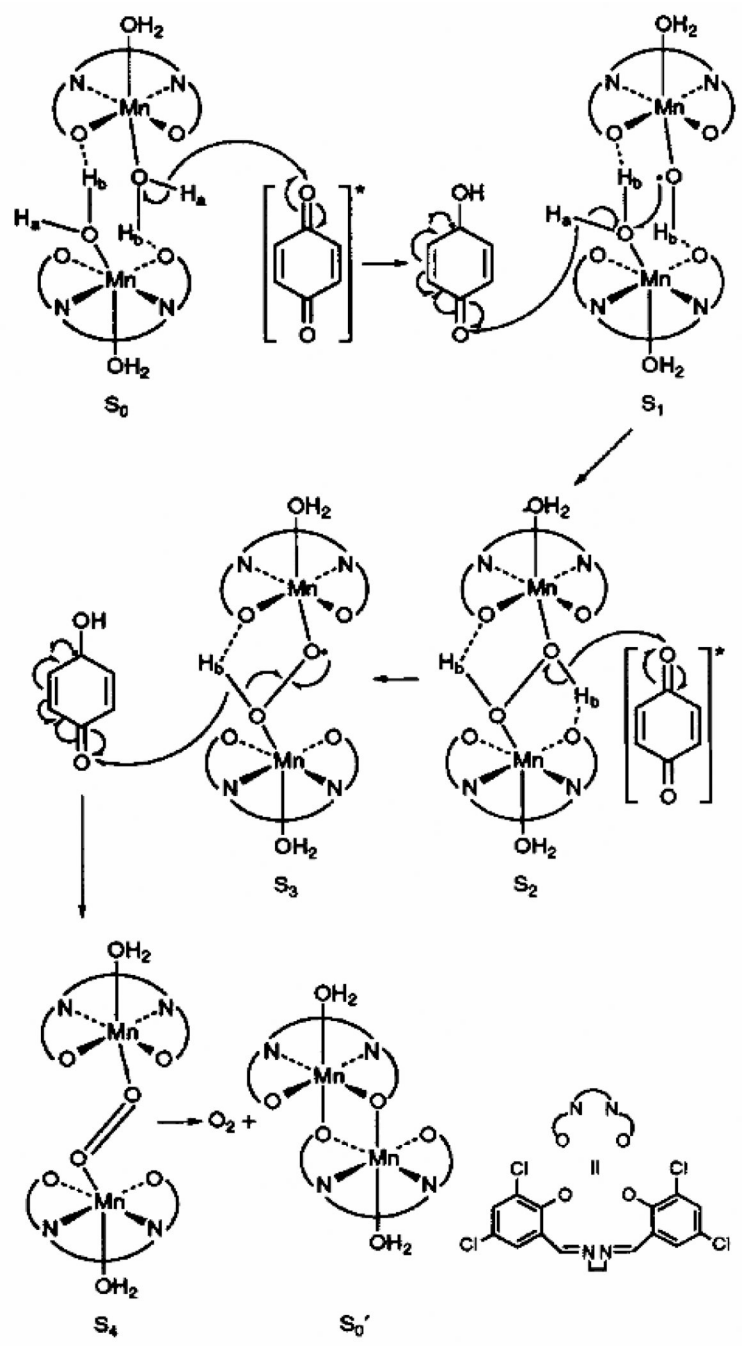

Figure 8.
Proposed mechanism of water oxidation by the $[Mn(3,5\text{-Cl-salen})(H_2O)_2]_2$ complex (figure was reproduced from ref. [88], with permission of the copyright holders).

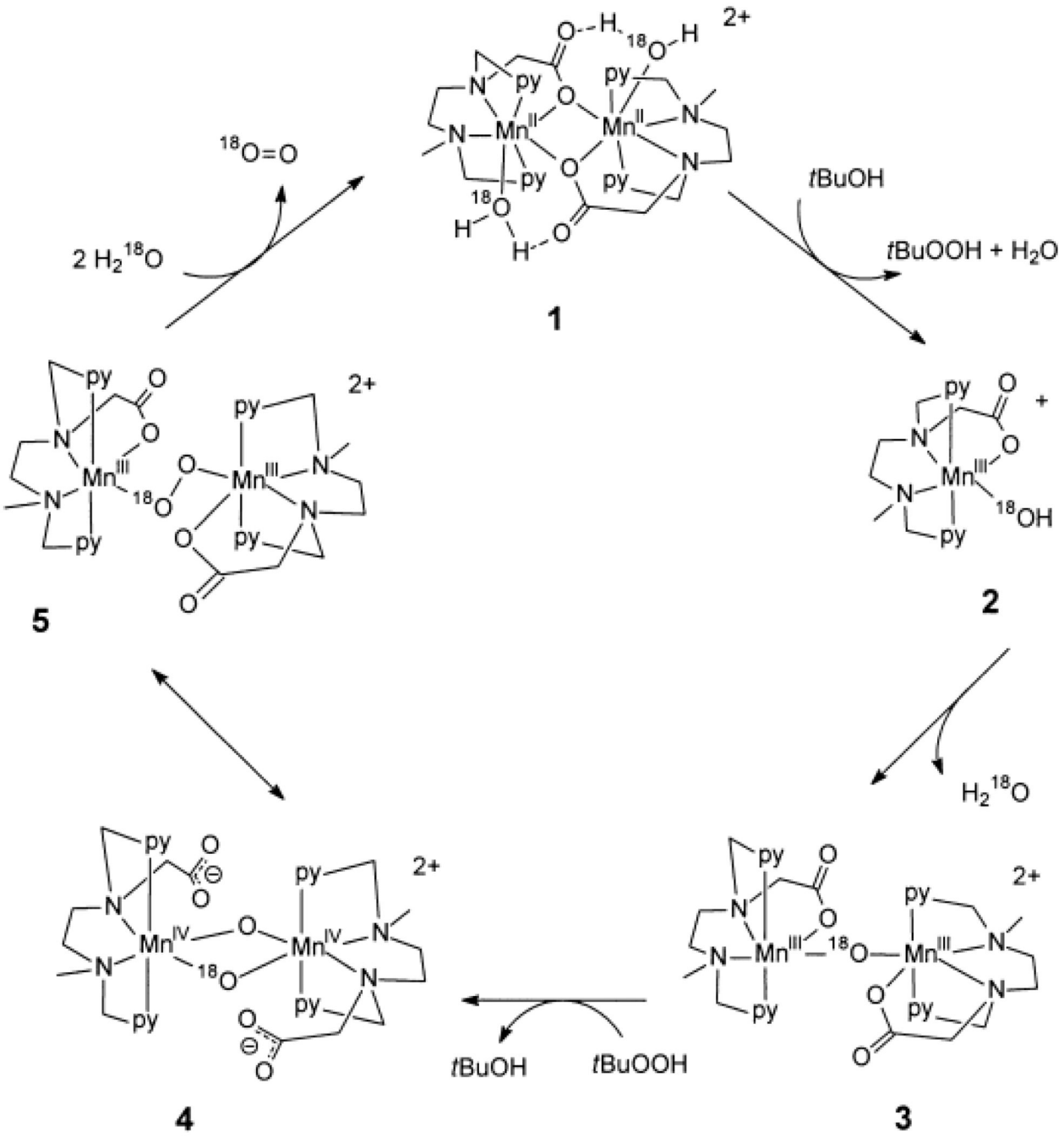

Figure 9.
Proposed mechanism of water oxidation by $[Mn^{II}_2(mcbpen)_2(H_2O)_2]^{2+}$ (**6**) using tert-butyl hydrogen peroxide as an oxidant (figure was reproduced from ref. [82], with permission of the copyright holders).

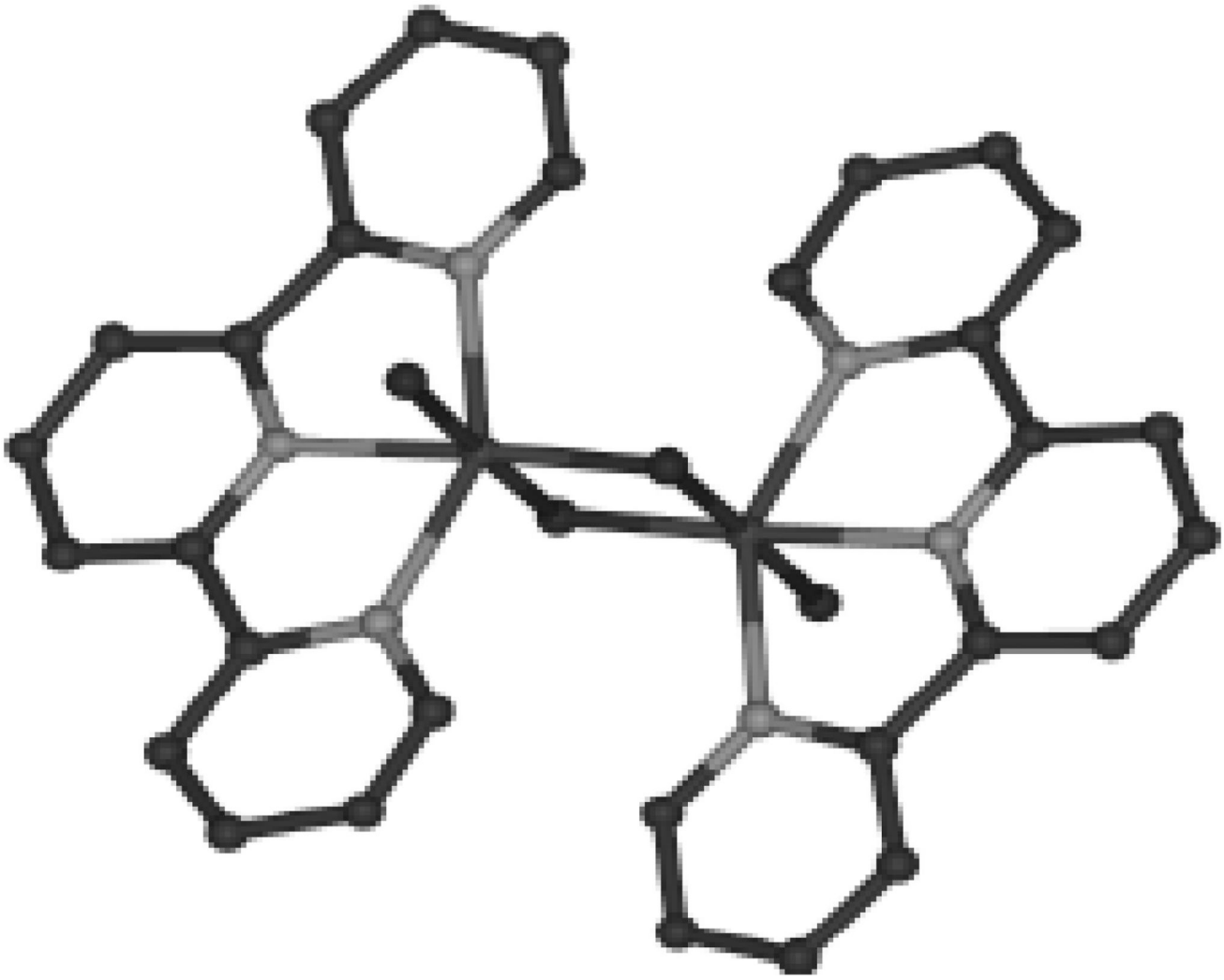

Figure 10.
Structure of **7**. Hydrogen atoms, nitrate counter ions and waters of crystallization are omitted for clarity.

Table 1

Oxygen evolution in natural and synthetic systems

Catalyst	k (s^{-1})	TON[a]	Oxidant	Reference
OEC	~40[b]	~60,000[c]	sunlight	[108,109]
1	0.0042	13.2	Ce(IV)	[75]
2	0.014	18.6	Ce(IV)	[73]
3	0.00077	3200	Ce(IV)	[74]
4	0.00035	580	Ce(IV)	[74]
6		10–20	TBHP	[82]
7		~1	Ce(IV)	[96]
7	0.0033	4	NaOCl	[83,93,110]
7	0.672	>50	HSO_5^-	[93,111]
Ru Red	0.051	75	Ce(IV)	[16,55]

[a] Turn Over Number

[b] Calculated from a maximum rate of O_2 evolution of ~ 800 μmol O_2/mg chl hr for a PSII membrane preparation.

[c] Calculated from an average exposure of 10^7 photons per PSII for inactivation.